Acetaldehyde Production in the Direct Ethanol Fuel Cell: Mechanistic Elucidation by Density Functional Theory

ARTICLE *in* THE JOURNAL OF PHYSICAL CHEMISTRY C · MARCH 2012

Impact Factor: 4.77 · DOI: 10.1021/jp210789s

5 AUTHORS, INCLUDING:

Xiaoming Cao
East China University of Science and Technology
22 PUBLICATIONS **342** CITATIONS

SEE PROFILE

Wen-Feng Lin
Loughborough University
62 PUBLICATIONS **1,460** CITATIONS

SEE PROFILE

THE JOURNAL OF PHYSICAL CHEMISTRY C

Article

pubs.acs.org/JPCC

Acetaldehyde Production in the Direct Ethanol Fuel Cell: Mechanistic Elucidation by Density Functional Theory

Richard Kavanagh, Xiao-Ming Cao, Wenfeng Lin,* Christopher Hardacre, and P. Hu*

School of Chemistry and Chemical Engineering, The Queen's University of Belfast, Belfast BT9 5AG, United Kingdom

ABSTRACT: This study employs density functional theory (DFT) calculations to examine the mechanism by which acetaldehyde is formed on platinum in a typical direct ethanol fuel cell (DEFC). A pathway is found involving the formation of a strongly hydrogen-bonded complex between adsorbed ethanol and the surface hydroxyl (OH) species, followed by the facile α-dehydrogenation of ethanol, with spontaneous weakening of the hydrogen bond in favor of adsorbed acetaldehyde and water. This mechanism is found to be comparably viable on both the close-packed surface and the monatomic steps. Comparison of further reactions on these two sites strongly indicates that the steps act as net removers of acetaldehyde from the product stream, while the flat surface acts as a net producer.

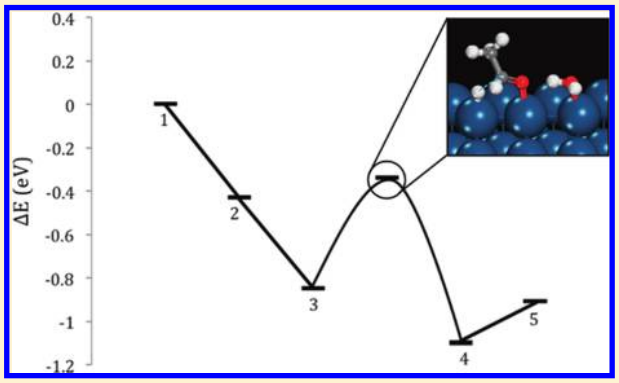

1. INTRODUCTION

Fuel cell technology offers one of the most tantalising prospects in the area of sustainable energy production, but significant scientific and technological difficulties remain to be solved before any such system can be viewed as truly viable in the real world. While many avenues of investigation are open in terms of the fuel employed in these cells, an efficient ethanol system could be viewed as the gold standard in terms of practicality and seamless integration into modern life. This is because sustainable ethanol production from biomass already exists on a vast scale, and it is relatively nontoxic and carries an exceptionally high energy density.[1−5] The high energy density arises from the 12-electron transfer from ethanol during complete oxidation to CO_2. However, the true efficiency of a DEFC is irrevocably linked to the selectivity of the anode catalyst toward CO_2 production, and this challenge has proved far from trivial to overcome.[6,7] To date, the main products that have been observed in real catalytic systems have been acetaldehyde (yielding only 2 electrons) and acetic acid (yielding only 4).[8−10] Of these, acetaldehyde production results in the lowest energy output and so is the least desirable. With this in mind, this study concentrates on understanding the process by which acetaldehyde is formed at the atomistic level as well as on the effect of the catalytically active site on the ultimate output of acetaldehyde into the product stream.

Several recent studies have worked toward the establishment of a mechanism for acetaldehyde production, both computationally[11−13] and spectroscopically,[14−16] but significant disparities remain between the theoretical understanding and what is practically observed. The current model strongly indicates that no traditional stepwise dehydrogenation pathway is kinetically viable under running conditions.[12] As such, a novel pathway is proposed involving the concerted removal of both α and hydroxyl hydrogens with the spontaneous desorption of acetaldehyde from the surface. This was supported by the isolation of a relatively low local energy maximum associated with the transition state and indicative of a more facile process.[11] While such a pathway is possible in principle, it is not wholly consistent with experimental data. It should be noted that further investigation revealed this pathway only to be the most facile on the (111) surface, with a stepwise dehydrogenation process commencing with α-CH dehydrogenation being preferred on the (211) and (100) surfaces.[12]

A key experimental observation arises from cyclic voltammetric spectroscopic studies, in which acetaldehyde formation is observed only to occur at potentials that are sufficiently high for the formation of surface oxidant species such as OH and O.[14,15] This result is experimentally ubiquitous and strongly indicates the direct involvement of such a species in acetaldehyde formation—an implication that cannot be readily explained in terms of the existing theoretical model. The second key experimental observation regards the effect of step density on selectivity, with highly step-dense catalysts producing markedly less acetaldehyde.[14] As such, it is important to examine both the majority (111) close packed surface of platinum and the common monatomic step defect.[17]

With all this in mind, the objectives of this work are as follows: (i) to elucidate a mechanism for acetaldehyde formation with the involvement of a surface oxidant species; (ii) to compare this mechanism in terms of kinetic and thermodynamic viability on the close-packed surface and the monatomic step; and (iii) to compare the viability of further reaction of acetaldehyde on these two sites.

Received: November 9, 2011
Revised: January 25, 2012
Published: February 28, 2012

2. COMPUTATIONAL DETAILS

All calculations reported here were conducted using the VASP package with the use of a plane wave basis set.[18−20] The generalized gradient approximation (GGA) was employed to describe the electron exchange and correlation terms with use of the PBE functional.[21] Electron−ion interactions are described using projector-augmented wave (PAW) potential.[22] The convergence of the plane-wave expansion was obtained with a cutoff energy of 400 eV. The ground state was determined using Methfessel−Paxton smearing of 0.05 eV.[23] Kinetic data were obtained using a constrained minimization transition state search technique.[24−26]

The close-packed surface was modeled as a (4 × 4) unit cell, while the monatomic step was modeled as a (3 × 1) (211) unit cell. For each surface the two-dimensional Brillouin integrations were fulfilled using a (3 × 3 × 1) Monkhorst−Pack grid.[27] The (211) surface provides the (100) monatomic step (generally regarded as being the most common defect on real platinum surfaces),[17,28] separated by (111) terraces. A four-layer slab was employed, with relaxation of the upper two layers and the lower two being in fixed geometry. Separation of slabs in the normal direction was provided with the use of a 12 Å vacuum region.

The total energy of all surface adsorbates measured relative to reactants in the gas phase were calculated using a modified version of an established literature method:[15]

$$\Delta E_x = E_{x/OH/sur} - E_{OH/sur} - E_e - (y - 6)(E_{H/sur} - E_{sur})$$

where ΔE_x is the chemisorption energy of species X (formula: $C_xH_yO_z$) in the presence of OH, and $E_{x/OH/sur}$, $E_{OH/sur}$, E_e, $E_{H/sur}$, and E_{sur} are the total energies of the surface with adsorbed species X in the presence of OH, the surface in the presence of OH, gas phase ethanol, the surface with adsorbed H, and the clean surface, respectively. It should be noted that, in some cases, hydrogen initially associated with the adsorbed species has been removed by OH to form an adsorbed water molecule. For consistency, such hydrogens are still considered as part of the adsorbed species.

Mechanistic elucidation was carried out in standard fashion, with a trial-and-error approach being employed. The total energies of the intermediates and transition states associated with a comprehensive range of relevant surface reactions were calculated, and the most thermodynamically and kinetically viable steps were reported. For cases in which several conceivable intermediate geometries were possible, all such geometries were tested and the most stable were employed. Note that all calculations were carried out under vacuum conditions. While it is anticipated that the presence of the aqueous phase will have a measurable effect on the values presented, the model presented here facilitates direct comparison with existing literature data.[11,12]

3. RESULTS AND DISCUSSION

3.1. Hydrogen Bonding between Ethanol and Surface Hydroxyl Species. The application of an electrical potential to the catalytic surface results in the dehydrogenation of adsorbed water to form surface OH and O species, and it is these species that are the active oxidants in the system.[29] In order to determine the effect of these surface oxidants on the reaction, the interaction between adsorbed ethanol and surface OH was investigated. The results showed strong hydrogen bonding between the two species through the ethanol hydroxyl hydrogen, resulting in the formation of a complex species with marked thermodynamic stabilization. This occurs on both the (111) and (211) surfaces, and the energetic data (Table 1)

Table 1. Calculated Energetic Data for the Formation of H-Bonded Complexes between Ethanol and Surface OH[a]

ΔE (eV)	(111)	(211)
$CH_3CH_2OH_{(ads)}$ + $OH_{(ads)}$	−0.37	−0.43
$CH_3CH_2OH{-}OH_{(ads)}$	−0.95	−0.85

[a] ΔE values reported for adsorbed species are relative to CH_3CH_2OH in the gas phase and the catalytic surface in the presence of $OH_{(ads)}$, in which $CH_3CH_2OH_{(ads)}$ + $OH_{(ads)}$ was calculated with a large distance between $CH_3CH_2OH_{(ads)}$and $OH_{(ads)}$ in the same unit cell, while $CH_3CH_2OH{-}OH_{(ads)}$ was calculated in the same unit cell with small a distance between $CH_3CH_2OH$and $OH_{(ads)}$. In other words, there is no direct chemical bonding between $CH_3CH_2OH_{(ads)}$ and $OH_{(ads)}$ in $CH_3CH_2OH_{(ads)}$ + $OH_{(ads)}$, while $CH_3CH_2OH{-}OH_{(ads)}$ is effectively an adsorbed hydrogen bonded complex (see Figure 1).

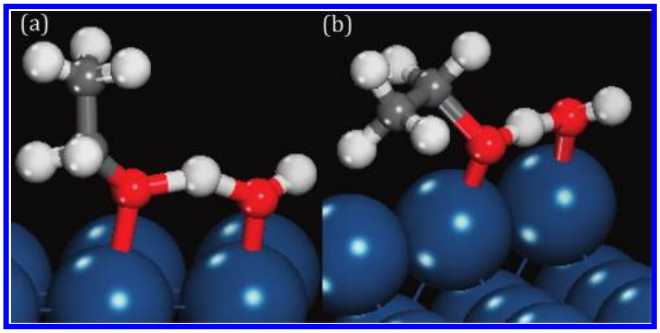

Figure 1. $CH_3CH_2OH{-}OH$ complex species on (a) the (111) surface and (b) the (211) surface.

and species geometries (Figure 1) are shown below. Note that this effect is not observed with surface O, with the presence of this species merely acting to sterically hinder adsorption of ethanol.

On the (111) surface, a highly facile hydrogen transfer process was observed, with the species moving between an ethanol−hydroxyl state and an ethoxyl−water state. The ΔE for this reaction was calculated to be only −0.01 eV, with an E_a of only 0.04 eV, and so the real system exists in rapid equilibrium. In the case of the (211) surface, no ethanol−hydroxyl state could be calculated as the system converged spontaneously to the ethoxyl−water state.

3.2. Pathway of Acetaldehyde Formation. The pathway for acetaldehyde is similar on the two surfaces studied. On the (111) surface, adsorption of ethanol is followed by the formation of the ethanol− hydroxyl complex, which exists in rapid equilibrium with the previously described ethoxyl−water complex state as follows:

$$CH_3CH_2OH{-}OH \rightleftharpoons CH_3CH_2O{-}H_2O$$

In fact, ΔE for this equilibrium is so small, and the energy barrier associated with it so low, that it can be described as a dynamic system, lacking a single, well-defined geometry, in which the initial and final states coexist with virtually equal probability.

dx.doi.org/10.1021/jp210789s | J. Phys. Chem. C 2012, 116, 7185−7188

This dynamic system can then undergo a reasonably facile α-dehydrogenation, with the transfer of the CH hydrogen to the catalytic surface. The concurrent result is the collapse of the dynamic system to a more static final state $CH_3CHO{-}H_2O$. In chemical terms, the removal of the α-hydrogen has significantly weakened the bond strength between the aldehyde O and the hydrogen-bonding H, resulting in the formation of acetaldehyde and water.

Hydrogen bonding between these species is weak and does not significantly inhibit desorption. The calculated pathway for the (211) surface proceeds in the same way, with the exception that the surface species proceed directly to the ethoxyl−water state following the adsorption of ethanol. The energetic data for these pathways are given below (Table 2) and shown in the form of pathway diagrams (Figures 2 and 3).

Table 2. Energetic and Kinetic Data for the Complete Pathway of Acetaldehyde Formation on the (111) and (211) Surfaces[a]

	(111)		(211)	
	ΔE (eV)	E_a (eV)	ΔE (eV)	E_a (eV)
$CH_3CH_2OH_{(g)} + OH_{(ads)}$	0		0	
$CH_3CH_2OH_{(ads)} + OH_{(ads)}$	−0.37		−0.43	
$CH_3CH_2OH{-}OH_{(ads)}$	−0.95			
$CH_3CH_2O{-}H_2O_{(ads)}$	−0.96	0.04	−0.85	
$CH_3CHO\text{-}H_2O_{(ads)}$	−1.00	0.41	−1.10	0.51
$CH_3CHO + H_2O_{(ads)}$	−0.90		−0.91	

[a] ΔE values reported for adsorbed species are relative to the total energy of CH_3CH_2OH in the gas phase and the catalytic surface in the presence of adsorbed OH. X + Y (X = $CH_3CH_2OH_{(g)}$, $CH_3CH_2OH_{(ads)}$, and CH_3CHO; Y = $OH_{(ads)}$ and $H_2O_{(ads)}$) indicates that there is no direct chemical bonding between X and Y, while X−Y represents an adsorbed hydrogen-bonded complex (also see the table caption of Table 1). The total energy of $CH_3CH_2OH_{(g)} + OH_{(ads)}$ is set zero as the reference.

The first, and perhaps most important, inference that can be made from these data is that the involvement of the surface OH species results in a significantly more facile process than the traditional stepwise processes found in the existing theoretical literature (calculated as having an initial barrier of 0.65 eV.)[11] Given that acetaldehyde is the major product of most real platinum-based systems, this is in good agreement with experimental evidence and, furthermore, explains the fact that acetaldehyde formation is only observed at relatively high running potentials.

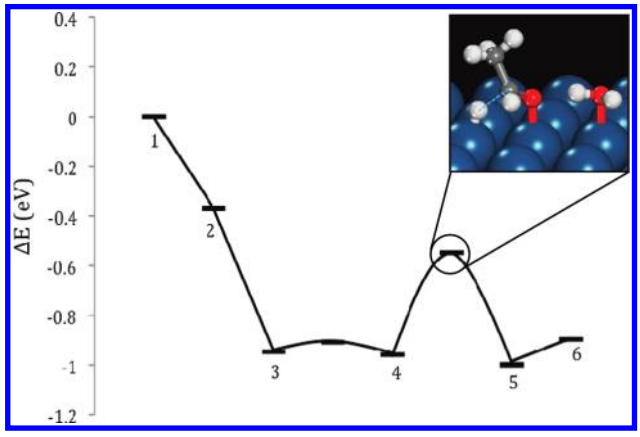

Figure 2. Complete pathway for acetaldehyde formation on (111) surface. 1, $CH_3CH_2OH_{(g)} + OH_{(ads)}$; 2, $CH_3CH_2OH_{(ads)} + OH_{(ads)}$; 3, $CH_3CH_2OH{-}OH_{(ads)}$ complex; 4, $CH_3CH_2O{-}H_2O_{(ads)}$ complex; 5, $CH_3CHO{-}H_2O_{(ads)}$ complex in the presence of H; 6, $CH_3CHO_{(ads)} + H_2O_{(ads)}$ in the presence of H. Inset: transition state associated with α-dehydrogenation.

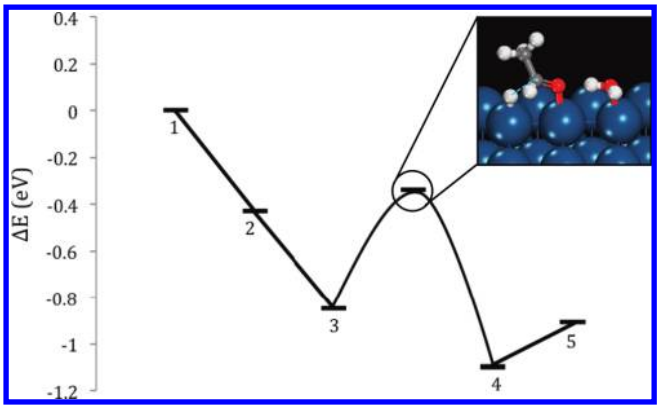

Figure 3. Complete pathway for acetaldehyde formation on (211) surface: 1, $CH_3CH_2OH_{(g)} + OH_{(ads)}$; 2, $CH_3CH_2OH_{(ads)} + OH_{(ads)}$; 3, $CH_3CH_2O{-}H_2O_{(ads)}$ complex; 4, $CH_3CHO{-}H_2O_{(ads)}$ complex in the presence of H; 5, $CH_3CHO_{(ads)} + H_2O_{(ads)}$ in the presence of H. Inset: transition state associated with α-dehydrogenation.

Comparison of the two pathways indicates that the process is somewhat more viable on the (111) surface than the (211) surface—both thermodynamically and kinetically. While this would appear to be in good agreement with the observation that step-dense catalysts produce less acetaldehyde, it must be noted that, at typical running potentials, the oxidant coverage on the (211) surface is significantly higher than on the (111) surface[25] and, as such, the effective rate of the reaction is likely higher on the (211) surface. In order to explain this apparent discrepancy, the viability of further reaction of acetaldehyde on the two surfaces must be considered.

3.3. Dehydrogenation of Acetaldehyde. The dehydrogenation of acetaldehyde to form the acetyl species is an exceptionally facile reaction on both surfaces, having an energy barrier of 0.11 eV on the (111) surface and of 0.15 eV on the (211) surface. However, of key importance are the adsorption energies of acetaldehyde on the two surfaces. The adsorption energy on the (111) surface is only −0.15 eV, indicating a virtually spontaneous desorption process, while it is −0.71 eV on the (211) surface. This large difference in adsorption energies, and the resulting difference in residence times, results in a system in which any acetaldehyde produced on the (211) surface undergoes rapid reaction to the form the acetyl species, while acetaldehyde produced by the (111) surface is almost immediately lost to the product stream. It is also conceivable for it to adsorb onto the (211) surface and be reacted further there. It is worth noting that the existing theoretical model predicts that the acetyl species can react further to form acetic acid or CO.[12] As such, the model presented here predicts that the close-packed surface acts as a net producer of acetaldehyde, while the monatomic steps act as a net remover of the species from the product stream. This is in good agreement with experimental observations.[14]

It is important to note that, while this work represents an important step toward developing a truly realistic model of this complex electrocatalytic system, it does not consider the effects of the solvent medium. It has been shown in previous

dx.doi.org/10.1021/jp210789s | J. Phys. Chem. C 2012, 116, 7185−7188

theoretical investigations that explicit inclusion of the aqueous phase can have a significant impact, both on the absolute energetic values presented and on the resulting physical implications.[30] While the solvent effect on the α-dehydrogenation is currently under investigation in our group, the results presented here provide a basis upon which more complete understanding of the system can be built.

4. CONCLUSION

The complete pathways of acetaldehyde formation were elucidated for both the close-packed platinum surface and the monatomic step, with involvement of the surface OH species in each case. The reaction was found to proceed via the formation of a complex hydrogen-bonded species that is highly thermodynamically stable with respect to isolated adsorbed ethanol and OH species. This complex exists in rapid equilibrium between ethanol−hydroxyl and ethoxyl−water forms, with the two forms being of almost identical thermodynamic stability. Subsequent to complexation, α-dehydrogenation occurs, resulting in a thermodynamic shift in favor of acetaldehyde and water. The reaction was found to be reasonably facile, in good agreement with experimental evidence.

Comparison of the adsorption energies of acetaldehyde on the two sites indicates a large difference in the residence times of the adsorbed species. When coupled with the availability of a facile acetaldehyde dehydrogenation pathway on both sites, this results in a marked difference in the degree of further reaction, leading to the action of the close-packed surface as a net producer of acetaldehyde and the action of the monatomic steps as net removers of the species from the product stream in agreement with experimental evidence.

■ AUTHOR INFORMATION

Notes

The authors declare no competing financial interest.

■ ACKNOWLEDGMENTS

This work was supported by the EPSRC (TS/H001875/1), Johnson Matthey plc., and the Technology Strategy Board. Thanks go, for many useful discussions, to Drs David Thompsett, Jonathan Sharman, and Alex Martinez from Johnson Matthey.

■ REFERENCES

(1) Lynd, L. R. *Annu. Rev. Energy Environ.* **1996**, *21*, 403−465.
(2) Carrette, L.; Friedrich, K. A.; Stimming, U. *Fuel Cells* **2001**, *1*, 5−39.
(3) Song, S.; Tsiakaras, P. E. *Appl. Catal., B* **2006**, *63*, 187−193.
(4) Tsiakaras, P. E. *J. Power Sources* **2007**, *171*, 107−112.
(5) Fujiwara, N.; Friedrich, K. A.; Stimming, U. *J. Electroanal. Chem.* **1999**, *472*, 120−125.
(6) Vigier, F.; Rousseau, S.; Coutanceau, C.; Leger, J. M.; Lamy, C. *Top. Catal.* **2006**, *40*, 111−121.
(7) Colmenares, L.; Wang, H.; Jusys, Z.; Jiang, L.; Yan, S.; Sun, G. Q.; Behm, R. J. *Electrochim. Acta* **2006**, *52*, 221−233.
(8) Nonaka, H.; Matsumura, Y. *J. Electroanal. Chem.* **2002**, *520*, 101−110.
(9) Hitmi, H.; Belgsir, E. M.; Leger, J. M.; Lamy, C. R.; Lezna, O. *Electrochim. Acta* **1994**, *39*, 407−415.
(10) Gootzen, J. F. E.; Visscher, W.; van Veen, J. A. R. *Langmuir* **1996**, *12*, 5076−5082.
(11) Wang, H. F.; Liu, Z. P. *J. Phys. Chem. C* **2007**, *111*, 12157−12160.
(12) Wang, H. F.; Liu, Z. P. *J. Am. Chem. Soc.* **2008**, *130*, 10996−11004.
(13) Choi, Y. M.; Liu, P. *Catal. Today* **2011**, *165*, 64−70.
(14) Wang, H.; Jusys, Z.; Behm, R. J. *J. Phys. Chem. B* **2004**, *108*, 19413−19424.
(15) Colmati, F.; Tremiliosi-Filho, G.; Gonzalez, E. R.; Berná, A.; Herrero, E.; Feliu, J. M. *Faraday Discuss.* **2008**, *140*, 379−397.
(16) Heinen, M.; Jusys, Z.; Behm, R. J. *J. Phys. Chem. C* **2010**, *114*, 9850−9864.
(17) Liu, Z. P.; Hu, P. *J. Am. Chem. Soc.* **2003**, *125*, 1958−1967.
(18) Kresse, G.; Hafner, J. *Phys. Rev. B* **1993**, *47*, 558−561.
(19) Kresse, G.; Hafner, J. *Phys. Rev. B* **1993**, *48*, 13115−13118.
(20) Kresse, G.; Hafner, J. *Phys. Rev. B* **1993**, *49*, 14251−14269.
(21) Perdew, J. P.; Burke, K.; Ernzerhof, M. *Phys. Rev. Lett.* **1996**, *77*, 3865−3868.
(22) Blochl, P. *Phys. Rev. B* **1994**, *50*, 17953−17979.
(23) Methfessel, M.; Paxton, A. T. *Phys. Rev. B* **1989**, *40*, 3616−3621.
(24) Alavi, A.; Hu, P.; Deutsch, T.; Sylvestrelli, P. L.; Hutter, J. *Phys. Rev. Lett.* **1998**, *80*, 3650−3653.
(25) Michaelides, A.; Hu, P. *J. Am. Chem. Soc.* **2000**, *122*, 9866−9867.
(26) Michaelides, A.; Hu, P. *J. Am. Chem. Soc.* **2001**, *123*, 4235−4242.
(27) Monkhorst, H. J.; Pack, J. D. *Phys. Rev. B* **1976**, *13*, 5188−5192.
(28) Fang, Y. H.; Liu, Z. P. *J. Phys. Chem. C* **2009**, *113*, 9765−9772.
(29) Rossmeisl, J.; Nørskov, J. K.; Taylor, C. D.; Janik, M. J.; Neurock, M. *J. Phys. Chem. B* **2006**, *110*, 21833−21839.
(30) Kavanagh, R.; Cao, X. M.; Lin, W. F.; Hardacre, C.; Hu, P. *Angew. Chem., Int. Ed.* **2012**, DOI: 10.1002/anie.201104990.